ANNALS of Clinical and Translational Neurology
Open Access
ANA American Neurological Association since 1875

RESEARCH ARTICLE

Depdc5 knockdown causes mTOR-dependent motor hyperactivity in zebrafish

Hortense de Calbiac[1,4], Adriana Dabacan[2], Elise Marsan[1], Hervé Tostivint[3], Gabrielle Devienne[1], Saeko Ishida[1], Eric Leguern[1], Stéphanie Baulac[1], Raul C. Muresan[2], Edor Kabashi[1,4] & Sorana Ciura[1,4]

[1]Sorbonne Universités Paris VI, UMR CNRS 1127 UPMC, INSERM U 1127, CNRS, UMR 7225, Institut du Cerveau et de la Moelle épinière – ICM, Paris, France
[2]Transylvanian Institute of Neuroscience (TINS), Str. Ploiesti 33, Cluj-Napoca 400157, Romania
[3]Evolution des Régulations Endocriniennes, UMR 7221, CNRS and Muséum National d'Histoire Naturelle, Paris, France
[4]Current address: Institut Imagine, UMR Inserm 1163, University Paris Descartes, Hospital Necker-Enfants Malades, 24 Boulevard du Montparnasse, Paris 75015, France

Correspondence
Sorana Ciura, Institut du Cerveau et de la Moelle Epinière (ICM), 47 Boulevard de l'Hopital, 75013, Paris, France.
Tel: ++33157274312; Fax: ++33157274027;
E-mail: sorana.ciura@icm-institute.org

Funding Information
Funding for this work was received from the Fédération pour la Recherche sur le Cerveau (FRC SB and EK), AFM-Téléthon (18469 and 21488 for SC and 18462 for EK). Also support from a grant from Consiliul National al Cercetarii Stiintifice (CNCS) - ˇUnitatea Executiva pentru Finantarea Invatamantului Superior, a Cercetarii Dezvoltarii si Inovariiˇ (UEFISCDI) (RM), and the program "Investissements d'avenir" ANR-10-IAIHU-06 was obtained. HC (PLP20141031462) and EM (FDT20160736468) obtained PhD awards by the Fondation pour la Recherche Medicale.

Received: 17 January 2018; Accepted: 18 January 2018

Annals of Clinical and Translational Neurology **2018; 5(5): 510–523**

doi: 10.1002/acn3.542

Abstract

Objective: *DEPDC5* was identified as a major genetic cause of focal epilepsy with deleterious mutations found in a wide range of inherited forms of focal epilepsy, associated with malformation of cortical development in certain cases. Identification of frameshift, truncation, and deletion mutations implicates haploinsufficiency of *DEPDC5* in the etiology of focal epilepsy. DEPDC5 is a component of the GATOR1 complex, acting as a negative regulator of mTOR signaling. **Methods**: Zebrafish represents a vertebrate model suitable for genetic analysis and drug screening in epilepsy-related disorders. In this study, we defined the expression of *depdc5* during development and established an epilepsy model with reduced Depdc5 expression. **Results**: Here we report a zebrafish model of Depdc5 loss-of-function that displays a measurable behavioral phenotype, including hyperkinesia, circular swimming, and increased neuronal activity. These phenotypic features persisted throughout embryonic development and were significantly reduced upon treatment with the mTORC1 inhibitor, rapamycin, as well as overexpression of human WT *DEPDC5* transcript. No phenotypic rescue was obtained upon expression of epilepsy-associated *DEPDC5* mutations (p.Arg487* and p.Arg485Gln), indicating that these mutations cause a loss of function of the protein. **Interpretation**: This study demonstrates that Depdc5 knockdown leads to early-onset phenotypic features related to motor and neuronal hyperactivity. Restoration of phenotypic features by WT but not epilepsy-associated Depdc5 mutants, as well as by mTORC1 inhibition confirm the role of Depdc5 in the mTORC1-dependent molecular cascades, defining this pathway as a potential therapeutic target for *DEPDC5*-inherited forms of focal epilepsy.

Introduction

Focal seizures, which originate within neuronal networks limited to one brain hemisphere,[1] are the most frequent epilepsies. In 2013, the discovery of mutations in the negative regulator of mTOR complex 1 (mTORC1), *DEPDC5* (DEP domain containing protein 5) in autosomal-dominant familial focal epilepsy has open novel perspectives in the field.[2,3] *DEPDC5* mutations have also been identified in cases with a wide range of clinical features associated with focal epileptic disorders, including nocturnal frontal lobe epilepsy (NFLE), temporal lobe epilepsy, (TLE) as

well as familial focal epilepsy with variable foci (FFEVF).[2–6] Furthermore, *DEPDC5* mutations have also been described more recently in patients with epileptic features associated with focal cortical dysplasia.[6–8] A large number of mutations spanning the coding sequence of *DEPDC5* have been identified in epilepsy-related disorders with the majority (approximately 80%) of these mutations causing premature codon termination.[9] In lymphoblastoid cell lines obtained from three patients that carried one of the several nonsense mutations identified, the p.Arg239*, p.Arg487*, and the p.Arg1087* *DEPDC5* mutations, were shown to be specifically degraded by the nonsense-mediated mRNA decay machinery,[2,4] indicating that focal epilepsy is related to *DEPDC5* haploinsufficiency.

DEPDC5 encodes a protein of 1603 amino acids, containing two recognizable domains involved in protein–protein interaction: DEP and DUF3964. It was recently characterized as an essential member of the GATOR1 (Gap Activity Toward Rags) molecular complex acting as a key negative regulator of the mTORC1.[10–13] Two other components of the GATOR1 complex, NPRL2 and 3 have been shown to be mutated in familial focal epilepsy with or without focal cortical dysplasia,[5,13–15] suggesting hyperactivation of mTORC1 as a major cause of epileptic syndromes. Rodent models of Depdc5 confirm the essential role played by this mTOR regulator in development.[12,16] DEPDC5 homozygous null mutations cause embryonic lethality at midgestation due to a range of abnormalities such as general hypoplasia, cranial dysplasia and cardiovascular defects. Interestingly, conditional knockout of Depdc5 in neurons resulted in enlarged brain size, dysplasic cell bodies, and sensitization to epileptogenic treatments.[17] In both mouse and rat models, Depdc5 loss-of-function was associated with increased mTOR activity. Constitutive DEPDC5 heterozygous null animals were viable and presented subtle alterations of electrographic activity[12]; however, they lacked overt behavioral phenotypes and seizures,[12,16] highlighting the complexity of the Depdc5 loss-of-function phenotype.

Simple animal models that lack the complex organization of the mammalian central nervous system and present stereotyped behaviors at early stages of development can provide a rapid readout of subtle defects in neuronal activity. Zebrafish in particular has recently emerged as a prominent vertebrate genetic model for epilepsy-related mutations[18,19] due to the relative ease of genetic manipulation, rapid development, and small size amenable to high-throughput screening methods. There is only one orthologue of *DEPDC5* in zebrafish; the level of identity of the zebrafish *depdc5* and human *DEPDC5* is 75%, with members of the mTOR pathway being equally well conserved (Table S1). Efforts to establish metrics of epileptic-like phenotypes in zebrafish have made significant headway. The first report of chemically induced seizures using the convulsant drug pentylenetetrazole (PTZ) documented stereotypical swimming abnormalities in 1-week-old larvae, consisting of circular trajectories, which correlated with increased synchronized neuronal activity in the zebrafish optic tectum as evidenced by field recordings.[20] Subsequent studies have successfully reproduced these effects in genetic models of epilepsy in zebrafish.[21–24] Recently, a zebrafish homozygous null model for the mTOR regulator protein, TSC2, was reported to display epileptiform activity and defective locomotion responses,[25] validating the use of this vertebrate model organism for epilepsies related to the mTOR pathway.

Here we develop a zebrafish model for *DEPDC5*-related epilepsies by knocking down the unique orthologue of DEPDC5 in this organism. We initially demonstrate that *depdc5* transcript is expressed in the brain of zebrafish embryos. Depdc5 knockdown resulted in hyperkinesia, aberrant locomotion and increased neuronal activity. We further demonstrate that two pathogenic mutations of DEPDC5, p.Arg487*, and the p.Arg485Gln, functionally inactivate the protein, as the respective transcripts were unable to compensate for the loss of function of the zebrafish orthologue, whereas the expression of human WT DEPDC5 significantly reduced the phenotype. Similarly, treatment with rapamycin, a well-known mTORC1 inhibitor, reduced aberrant locomotion resulting from *depdc5* knockdown. These results establish an mTORopathy model associated with epileptic-like features in zebrafish and provide functional data to support *DEPDC5* loss of function in patients carrying *DEPDC5* mutations.

Methods

Zebrafish Maintenance

Adult and larval zebrafish (Danio rerio) were maintained at the ICM (Institut du Cerveau et de la Moelle épinière, Paris) fish facility and bred according to the National and European Guidelines for Animal Welfare. Experiments were performed on wild-type embryos from AB and TL strains. Zebrafish were raised in a 28°C incubator in embryo water: 0.6 g/L aquarium salt (Instant Ocean, Blacksburg, VA) in reverse osmosis water +0.01 mg/L methylene blue. Experimental procedures were approved by the National and Institutional Ethical Committees. Embryos were staged in terms of hours post fertilization (hpf) at 28°C based on morphological criteria.[26]

Microinjection of oligonucleotides and cDNA into zebrafish embryos

Antisense Morpholino oligonucleotides (AMOs) (GeneTools Philomath, OR) were used to knockdown the

expression of the sole orthologue of the *DEPDC5* gene in zebrafish. The target for knockdown was the ATG of the *Depdc5* transcript (ATG-AMO sequence: 5′-TGCCTTCATGGTGACCHTCATTTTA-3′). A control AMO, containing five mismatch nucleotides and not binding anywhere in the zebrafish genome, was used to assess the specificity of the observed phenotype (5′-TGCgTTgATcGTGACCgTgATTTTA-3′). The splice blocking morpholino was used to target the intron 1 to exon 2 junction of the *depdc5* transcript (5′- ACATTCCTGTTT CACCATAGATGAT-3′). Working concentrations were established from dose-dependent toxicity curves for each of the AMOs and cDNAs described in this report. The optimal AMO concentration for injections was determined as the point on the toxicity curve where there was no significant increase in the percentage of morphologically deformed larvae. The ATG-blocking AMO was injected at a concentration of 0.4 mmol/L (3.37 ng/nL), whereas the splice AMO was injected at a concentration of 0.65 mmol/L(5.51 ng/nL). Human wild-type *DEPDC5* cDNA was obtained from Dharmacon (NM_001242897.1; Accession: BC144291 Clone ID: 9052811). Two epilepsy-related mutants, the nonsense p.Arg487* and the missense p.Arg485Gln *DEPDC5*[2,4] were generated by site-directed mutagenesis, cloned into the pcS2+ vector and linearized using the Not1 enzyme before being injected at 100 ng/uL. The microinjections were carried out at one cell stage.

In situ hybridization

To generate the Depdc5 probe, a 560 bp fragment of the zebrafish *depdc5* cDNA (XM_686358) was amplified by RT-PCR with primers as follows: 5′-AGGCTGTCAA TGGTTTCCTTT-3′ and 5′-GAAGAGTGGAACAGCGTG AAG-3′, then subcloned into pGEM-T easy (Promega, Charbonnières, France). Sense and antisense digoxigenin-labeled riboprobes were synthesized from the linearized plasmid with the RNA polymerases T7 or Sp6, using the RNA Labeling Kit (Roche Diagnostics, Mannheim, Germany). Embryo preparation and in situ hybridization was carried out as previously described in Quan et al.[27]

Motor activity analysis

To record global activity, 28 hpf zebrafish embryos in their chorion were placed on a plastic mesh (1.2 × 1.2 mm), submerged in embryo water and imaged using a Grasshopper digital camera (Point Gray) at the frequency of 30 fps. Global activity was measured using an automatized Zebralab system (ViewPoint, France). To record the number of coils (representing complete rotations of the embryo) and twitches (tail flicks), embryos were dechoryonated, placed in a 100 mm petri dish filled with embryo water and recorded using a Grasshopper digital camera (Point Gray) at 30 fps. The movements of each individual embryo were manually assessed. For touch-evoked escape response (TEER) measurements, zebrafish embryos that had not enclosed were manually dechoryonated and the morphology was assessed with a stereomicroscope. To perform the TEER test, embryos were placed in the middle of a petri dish with the diameter of 150 mm filled with embryo water at room temperature. Only morphologically normal embryos were used for this test, as even slight body curvatures can result in grossly impaired swimming parameters. A light touch to the tail with a plastic tip evoked a swimming episode, which was recorded with a Grasshopper digital camera (Point Gray) at 30 fps. The swimming trajectory was traced using the Manual tracking Plug-in (https://imagej.nih.gov/ij/plugins/manual-tracking.html) in ImageJ software (NIH). All the consecutive frames recorded from the onset to the end of the swimming episode were analyzed to obtain the x–y coordinates which were used for calculating the distance, velocity, and turning angle. The tortuosity of the trajectory was quantified as the average angle of deviation from a rectilinear trajectory, calculated frame by frame for the individual segments of the pathway projection.

96-well plates scoring for pharmacological modifiers

At 72 hpf, escape to touch responses were evaluated in a 96-well plate. Embryos were lightly touched on the tail with a plastic tip and a score was given according to their performance: 0– the embryo does not move at all. 1 – the embryo senses the touch but moves slightly staying in the center of the well. 2 – the embryo completes a full circle along the well after several stimulations. 3 – the embryo completes several full circles along the well after several stimulations. 4 – the embryo completes a full circle along the well after a single stimulation. 5 – the embryo completes several full circles along the well after a single stimulation.

In a 96-well plate, 24 hpf and 48 hpf embryos were incubated in rapamycin solution, with a final concentration of 0.5 and 1 μmol/L, respectively, until 72 hpf, when behavioral responses were assessed as described above.

Reverse-transcription PCR data

Total RNA from embryos was extracted using the TRIzol reagent (Invitrogen, Carlsbad, CA), following the provided protocol. RNA was quantified using the Nanodrop 8000 (Thermo Scientific, Waltham, MA) and its quality was checked using the 2100 Bioanalyzer (Agilent Technologies). cDNA was synthesized using Transcriptor Universal cDNA Master Mix (Roche, Basel, Switzerland). Primers pair

GGCAAACAAGTCCTACAAGCT and GAGCTCCACCAG ATCCAAAG amplified the sequence between exons 1 and 5. Primers specific for β-actin were used as a positive control. To test the efficacy of the splice-blocking morpholino, primer pairs GGCAAACAAGTCCTACAAGCT and TGCA GGTCCTCTTTCAAACTC were used to amplify a region between exons 1 and 3.

Electrophysiological analysis

Zebrafish larvae at 4–6 day post fertilization (dpf) were embedded in 1% agarose with the dorsal aspect facing upward. A glass electrode with a 2 μmol/L diameter aperture with resistance of 5–6 MΩ was filled with artificial cerebro-spinal fluid [HEPES 10 mmol/L, NaCl 134 mmol/L, KCl 2.9 mmol/L, $CaCl_2$ 2.1 mmol/L, $MgCl_2$ 1.2 mmol/L, glucose 10 mmol/L; pH 7.8]. This electrode was placed in the optic tectum and gap-free extracellular recordings were obtained in current clamp mode using a MultiClamp700B amplifier and a Digidata 1400 analog-to-digital interface (Molecular Devices). The extracellular field signal was acquired at a sampling rate of 1 kHz and downsampled to 250 Hz for analysis. For detecting depolarization events the signal was filtered with a band pass filter between 0.01 and 100 Hz postacquisition. Event detection was based on negative amplitude with a threshold set at -0.3 mV. The events were defined as distinct if there was at least a 4 sec time gap between threshold crossings. Their duration was computed as the time distance between the first and last threshold crossing. The height of the events was computed from the waveform of the raw extracellular signal, given by the difference between the minimum and maximum of the waveform for each event. Events were eliminated if the width was smaller than 40 msec. We compared the spontaneous activity between controls and Depdc5 knockdown zebrafish larvae from baseline recordings of 60 min duration. To verify that the preparation was intact and able to generate high-frequency neuronal discharges resembling the epileptiform activity, we then applied 20 mmol/L PTZ to chemically induce epileptiform-like electrographic activity.[20,28] To account for the variability in electrode placement and individual animals, we eliminated datasets that had outlying spontaneous activity (baseline activity outside two standard deviations of the mean) or where the application of PTZ had no effect on the electrographic activity. We define the total activity duration as the sum of all recorded events' duration within an hour.

Statistical analysis

Data were plotted and analyzed using the Excel software (Microsoft, Washington). Electrophysiological results were analyzed using the Clampfit software (Molecular Devices, California). One-way ANOVA test and the Bonferroni procedure were performed using SigmaStat (California) for determining statistically significant differences between experimental groups.

Results

Expression of the sole orthologue of *DEPDC5* during embryonic development in zebrafish

The zebrafish genome contains one orthologue of *DEPDC5* (*depdc5*; ENSDARG00000078105), sharing 75% identity with the human gene (ENSG00000100150; Table S1). A specific probe for the zebrafish *depdc5* mRNA (XM_686358) was designed and synthesized to determine the localization pattern of *depdc5* transcripts in zebrafish embryos. To characterize the expression of *depdc5*, we performed in situ hybridization analysis in whole-mounted 28 h post fertilization (hpf) zebrafish embryos. *depdc5* transcripts were found to be enriched specifically in the CNS (Fig. 1), with little to no signal detected in other structures (Fig. 1C). Within the CNS, strong levels of *depdc5* mRNA were detected in the telencephalon and midbrain regions, whereas the expression appeared to be reduced in the embryonic hindbrain and spinal cord of zebrafish (Fig. 1D). To determine the timeline of *depdc5* expression in the zebrafish development we analyzed the presence of the transcript by RT-PCR at several stages of embryonic and larval development, including 6, 24, 48, and 72 h postfertilization (Fig. 1E). We observed the presence of *depdc5* transcripts as early as 6 hpf, with the expression persisting at each of the stages of development measured in this study (Fig. 1E). These results suggest that during development, the expression of the zebrafish *DEPDC5* orthologue is enriched in the CNS.

Depdc5 knockdown leads to motor hyperactivity in zebrafish embryos

To study the effects of Depdc5 loss of function in zebrafish, we designed an antisense morpholino oligonucleotide (AMO) to bind to the initial ATG of the *depdc5* sequence and one control mismatch AMO. Zebrafish embryos exhibit early stereotyped motor activity starting at 17 hpf, consisting of repetitive twitches (tail flicks) and coils (complete rotations) at regular intervals, with frequencies varying in function of age as previously described.[29] At 28 hpf the frequency of these spontaneous activities is low, at <0.1 Hz, and supported by a synchronized, bilateral spinal circuit.[30] To determine if this early premotor activity presented abnormalit-

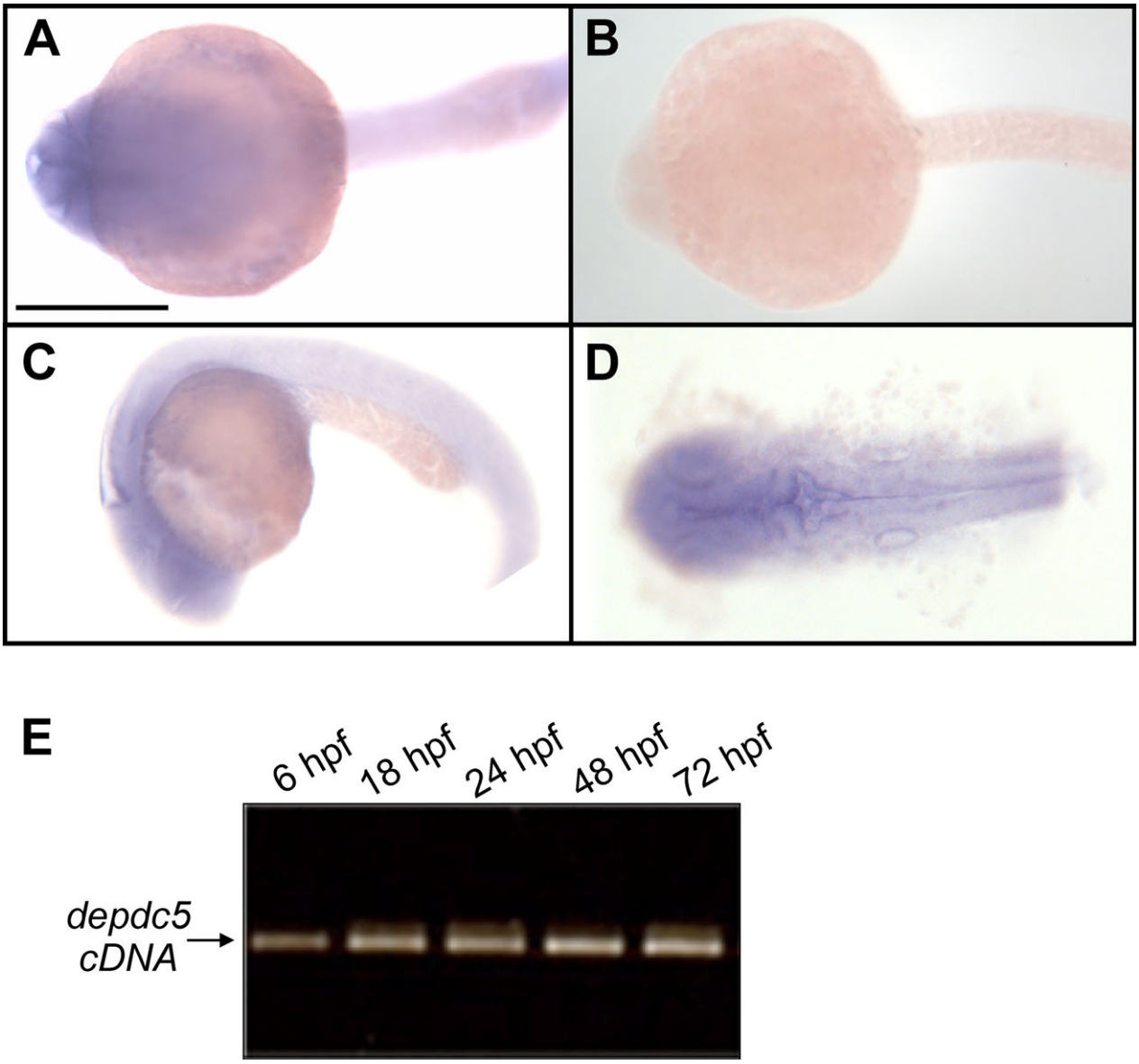

Figure 1. *depdc5* expression in early development in the zebrafish larva. (A) Ventral view of a 28 hpf embryo showing expression of the *depdc5* transcript in the telencephalon. (B) In situ hybridization using the control probe showing no positive signal. (C and D) Lateral and dorsal views, respectively, of the 28 hpf embryo showing the expression pattern in the brain and spinal cord. (E) RT-PCR detecting *Depdc5* expression in tissue obtained from zebrafish larvae at different stages of development.

ies in the Depdc5 knockdown condition, we employed automated monitoring of embryo movement inside the chorion. Quantification of total motor activity shows that Depdc5 knockdown larvae presented a hyperactive phenotype at this early developmental stage (Fig. 2A and B). Depdc5 knockdown larvae ($n = 100$) performed significantly more stereotypical movements when compared with fish injected with mismatch AMO ($n = 46$), as exemplified by full rotations (coils) (4.05 ± 0.69 coils/min vs. 1.32 ± 0.55 coils/min, respectively; $P = 0.039$) and tail flicks (twitches) (3.39 ± 1.19 twitches/min vs. 0.44 ± 0.21 twitches/min, respectively; $P = 0.011$). Therefore, while Depdc5 knockdown zebrafish maintained the ability to perform complex stereotyped behavior, they consistently triggered bursts of activity more often than in controls as quantified in Figure 2C. In addition, we observed hyperactivity displayed as recurrent uncontrollable tremors in a percentage ($26.9 \pm 4.26\%$) of Depdc5

knockdown zebrafish embryos (see Videos S1–S4). This type of activity was not observed in noninjected or mismatch AMO ($n = 46$) injected larvae.

Depdc5 loss of function causes aberrant locomotion and neuronal hyperactivity

We hypothesized that the motor hyperactivity assessed at early stages of development would lead to aberrant locomotion in Depdc5 knockdown zebrafish larvae at later stages. Spontaneous and PTZ-evoked epileptic-like phenotypes at this age have been previously linked to nonlinear swimming patterns and circling.[21,23] Zebrafish larvae develop escape responses to touch at 48 hpf, characterized by rectilinear swimming away from the stimulus. Touch-evoked escape responses (TEER) were used to quantify swimming velocity, distance, duration, as well as the trajectory tortuosity. Similar to previous studies reporting genetic and pharmacological models of epilepsy in zebrafish,[19] aberrant locomotion was characterized by tortuous, cork-screw swimming bouts (Fig. 3A). To quantify this phenotype of nonrectilinear swimming, we measured the turning angle between individual swimming segments in consequent video frames to determine the deviation from a straight line. As expected, this angle was significantly increased in the *depdc5* AMO-injected larvae as compared to controls (50.7 ± 2.14^{o}, $n = 102$ for depdc5 knockdown, vs. 25.3 ± 1.08^{o}, $n = 101$ for mismatch controls, $P < 0.001$; or vs. 26.5 ± 1.40^{o} for noninjected larvae, $n = 53$, $P < 0.001$; Fig 3C). At the same time, the total distance of the TEER trajectory was similar among all the conditions described above (data not shown) suggesting that *depdc5*

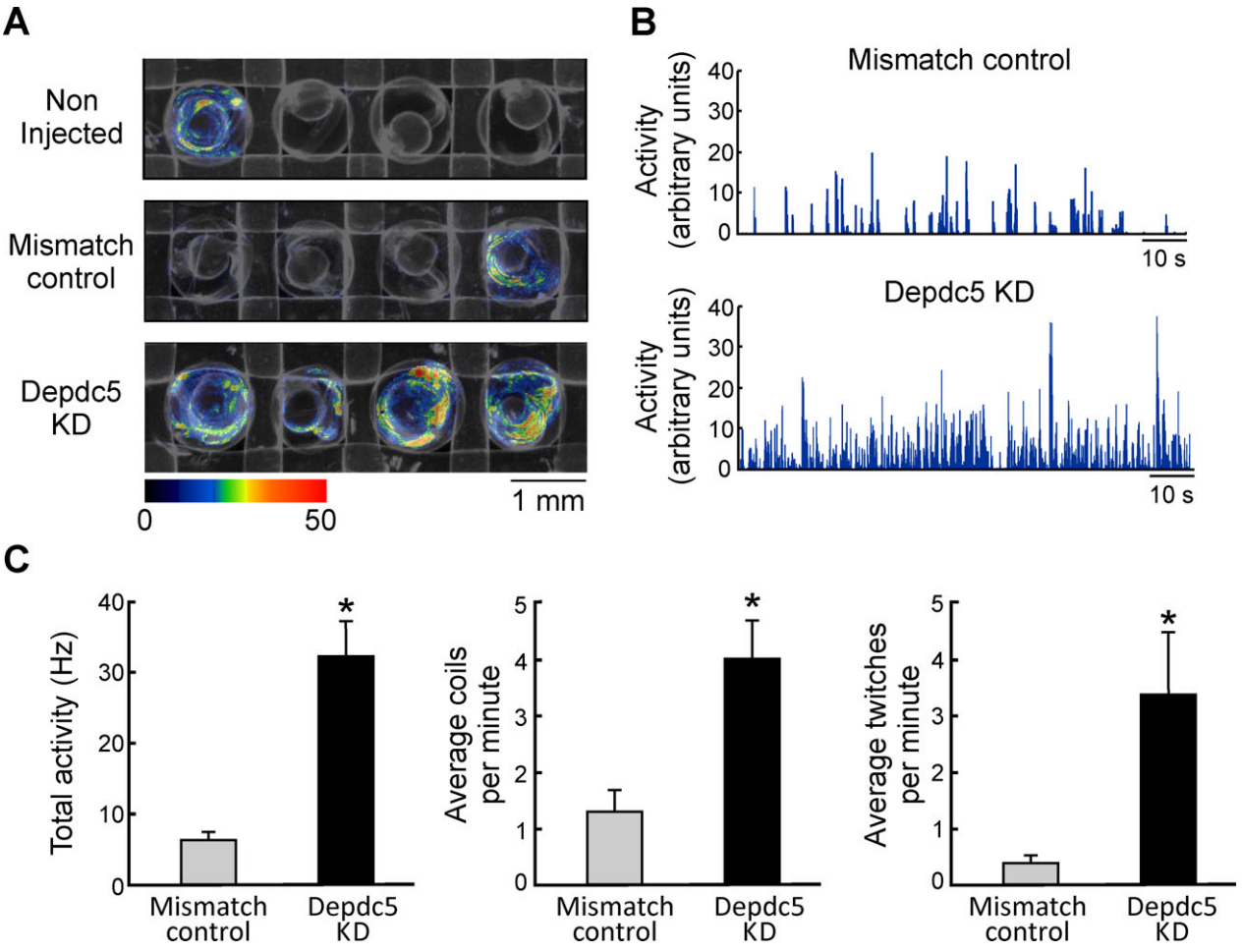

Figure 2. Depdc5 knockdown larvae show an early hyperactive motor phenotype. (A) Locomotor activity heatmap illustrating spontaneous movement in 28 hpf larvae inside the chorion over a period of 1 min showing an increase in general movement in the Depdc5 knockdown (KD) larvae as compared to mismatch and noninjected controls. (B) Parameters of the same activity showing increased frequency and amplitude of movement in Depdc5 KD animals. C. Quantification of total activity showing a significant hyperactive phenotype in the Depdc5 KD. Both the coiling and twitching frequency were significantly increased as compared to controls.

knockdown did not cause generalized locomotion impairment. Also, the embryo size and global appearance of the *depdc5* knockdown was similar to the noninjected or mismatch-injected zebrafish (Fig. S1). Similar percentages of developmentally delayed embryos were present in each of these groups. To further ascertain that these phenotypic features were not associated with generalized off-target morpholino toxicity, we used a splice blocking AMO targeting the intron 1/exon 2 junction, which caused abnormal splicing of the *depdc5* transcript (Fig. 3B). Abnormal splicing by the splice blocking AMO persisted in 5-day-old larvae (Fig. S1). Similar to the ATG-blocking AMO, injection of the splice AMO caused aberrant locomotion associated with significantly increased circular swimming following a TEER (53.5°±4.64; $n = 16$, $P < 0.001$ compared to mismatch; Fig. 3A). Moreover, a similar percentage of larvae with visible corkscrew-like swimming were observed upon injection with splice AMO as for the ATG-blocking AMO (75.9 ± 6.9% and 76.9 ± 3.9%, respectively; Fig. 3D). These results confirm that phenotypic features associated in zebrafish embryos were specifically due to Depdc5 knockdown.

The triggering and propagation of epileptic seizures in patients as well as in rodent models implicates increased synchronized neuronal depolarizations. To determine if the Depdc5 knockdown hyperactive phenotypic features were correlated with an increased neuronal electrical activity, extracellular field recordings were obtained from the optic tectum of agarose-embedded zebrafish larvae. Both control and Depdc5 knockdown larvae presented spontaneous neuronal activity bursts representing a summation of synchronized events (Fig. 4A). We found a significantly increased total duration of spontaneous neuronal activity in larvae injected with *depdc5* AMO when compared with mismatch AMO controls (52.9 ± 14.1 sec for Depdc5 knockdown vs. 14.6 ± 5.17 sec, for mismatch controls, $n = 9$ for both conditions, $P = 0.028$, Fig. 4B). Previous genetic models of epilepsy have shown increased sensitivity to PTZ application.[20,21,23,28,31] While both control and Depdc5 knockdown embryos showed significantly increased spontaneous basal activity in response to PTZ, we did not detect a difference in their respective sensitivity to the drug. Indeed, PTZ application resulted in proportionally equivalent increases of neuronal activity (214.62±0.55% in controls as compared to 215.16±0.72% for the Depdc5 knockdown embryos; $n = 9$ for both conditions; $P = 0.19$).

Epilepsy-causing mutations cause loss-of-function of *DEPDC5*

Furthermore, to confirm that hyperactive-related phenotypic features associated with aberrant locomotion were specifically due to Depdc5 knockdown, we performed rescue experiments where we introduced the human *DEPDC5* (h*DEPDC5*) cDNA alongside the translation blocking AMO. Animals that received WT h*DEPDC5* alone did not show an increased percentage of developmental or behavioral abnormalities, suggesting that the level of expression of this construct was not toxic to the zebrafish larvae (data not shown). At 48 hpf, coexpression of this gene alongside the translation blocking AMO resulted in a significant reduction in the Depdc5 knockdown phenotype (Fig 5A). Indeed, the trajectory of morphants coexpressing the h*DEPDC5* cDNA construct was significantly more rectilinear when compared with *depdc5* AMO-injected fish (25.2 ± 1.07°, $n = 55$ vs. 50.7 ± 2,14, $n = 102$, respectively; $P < 0.001$; Fig. 5B), and not different from mismatch controls (25.3 ± 1.08°, $n = 101$, $P = 0.96$). Overall, the percentage of fish exhibiting normal motor responses was significantly improved (4.79 ± 1.81% for Depdc5 knockdown vs. 49.5 ± 2.52% for Depdc5 knockdown + h*DEPDC5* WT; Fig. 5C), to a level similar to controls (89.9 ± 2.48% for noninjected and 87.7 ± 3.00% for mismatch controls). Mutant h*DEPDC5* were engineered by site-directed mutagenesis to introduce two different mutations described in focal epilepsy patients, p.Arg487* and p.Arg485Gln.[2,4] Overexpression of either h*DEPDC5*$^{p.Arg487*}$ or h*DEPDC5*$^{p.Arg485Gln}$ alone did not lead to any significant abnormalities of development, or deficits of swimming bouts performed at 48 h post fertilization (data not shown). Similarly, we did not notice any aberrant twitching or hyperactivity upon overexpression of these DEPDC5 mutations, indicating that the p.Arg487* and p.Arg485Gln variants are not associated with gain of function toxicity. However, as expected for loss-of-function mutations, coexpression of either h*DEPDC5*$^{p.Arg487*}$ or h*DEPDC5*$^{p.Arg485Gln}$ together with the *depdc5* ATG-blocking AMO failed to restore phenotypic features associated with Depdc5 knockdown in zebrafish, as both the swimming trajectory (illustrated in 5A and quantified in 5B) and percentage (Fig 5C) of affected fish were not significantly different from the AMO alone condition.

Inhibition of the mTORC1 by rapamycin rescues phenotypic features caused by *Depdc5* knockdown

DEPDC5 has been described as an essential part of the GATOR1 complex, an inhibitor of mTORC1.[10,12] In accordance with this, treatment of *depdc5* knockdown fish with the mTORC1 inhibitor, rapamycin, significantly improved the deviation angle of the swimming trajectory at 72 hpf (54.9 ± 5.99°, $n = 16$, for *depdc5* knockdown; vs. 28.5 ± 2.75°, $n = 12$, for *Depdc5* knockdown +

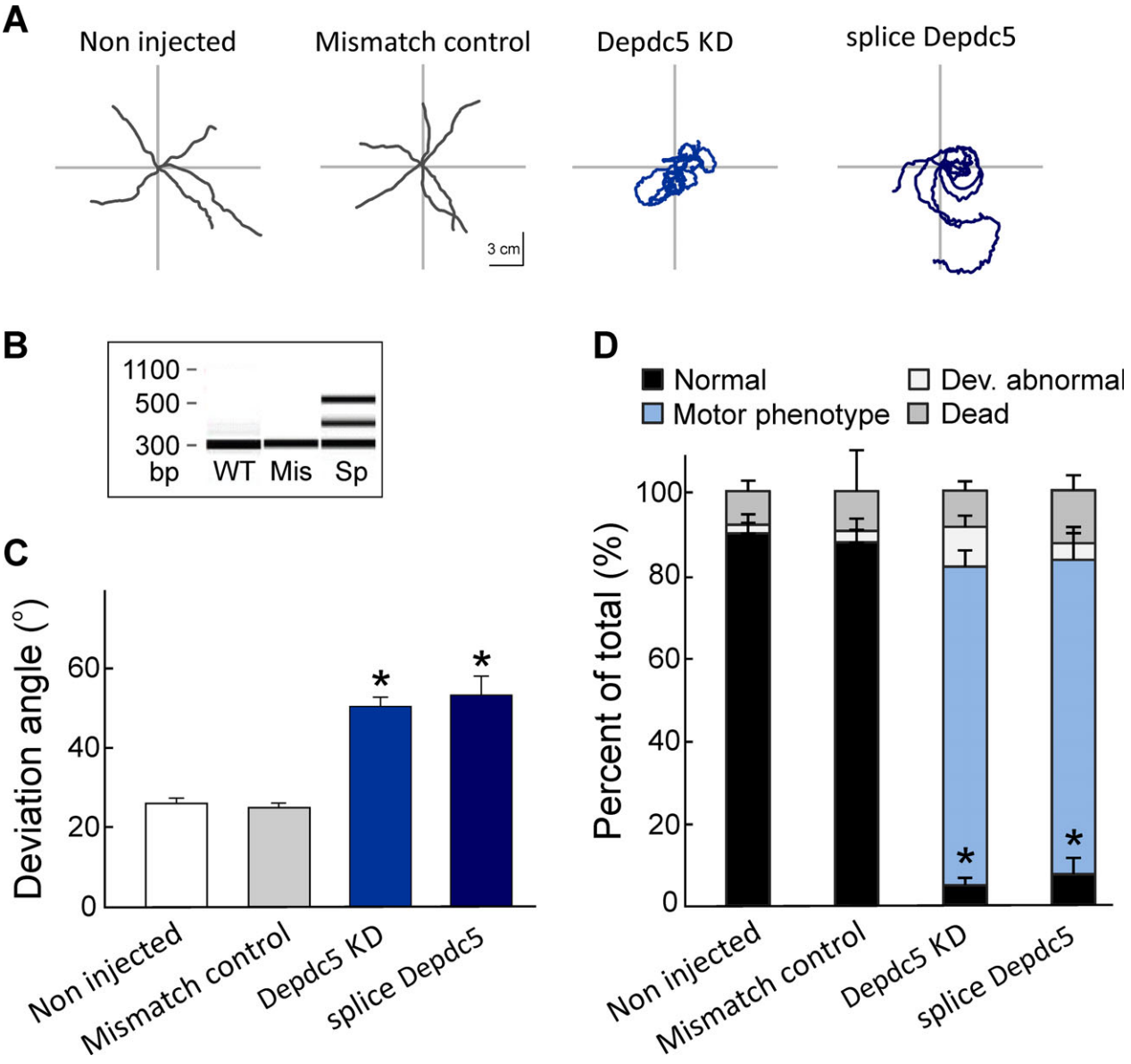

Figure 3. Depdc5 knockdown zebrafish exhibit a characteristic corkscrew-like swimming pattern. (A) Representative traces of individual swimming episodes at 48 hpf showing the typical tortuous trajectory of Depdc*5* knockdown fish as compared to noninjected and mismatch controls. Similar trajectories are described by the larvae injected with the ATG-targeting (Depdc5 KD) or splice-targeting (splice Depdc5) MO. (B) PCR product showing the effect of the splice MO on the *depdc5* transcript compared to noninjected (WT) or mismatch-injected (Mis) zebrafish. (C) The quantification of the tortuosity of the swimming trajectory measured as deviation angle shows significant differences between the *depdc5*-targeting morphants and the controls. (D) Stacked bar graph showing the distribution of phenotypes as a percentage of total larvae injected with *depdc5* ATG-targeting AMO (Depdc5 KD) or splice *depdc5* AMO as compared to noninjected or mismatch controls, including percentage of embryos that are developmentally affected/delayed. Significant increase in the percentage of larvae showing a motor phenotype (corkscrew-like swimming pattern) is observed only in the conditions targeting the *depdc5* transcript.

Rapamycin 0.5 μmol/L; $P = 0.002$) when the drug was administered starting at the 28 hpf stage. The effect of the drug was also assessed by scoring the TEER in a 96-well plate format, on a scale of 1–5 (see details in Materials and Methods). Aberrant locomotion as evidenced by the low motor score in Depdc5 knockdown was significantly improved by 44 h of rapamycin treatment (2.54 ± 0.14, $n = 65$, for Depdc5 knockdown + vehicle vs. 3.78 ± 0.17, $n = 59$, for Depdc5 knockdown + rapamycin 0.5 μmol/L; $P < 0.001$). To test whether treatment with rapamycin at a later stage of development would be able to modify the Depdc5 knockdown phenotype, we applied a higher dose

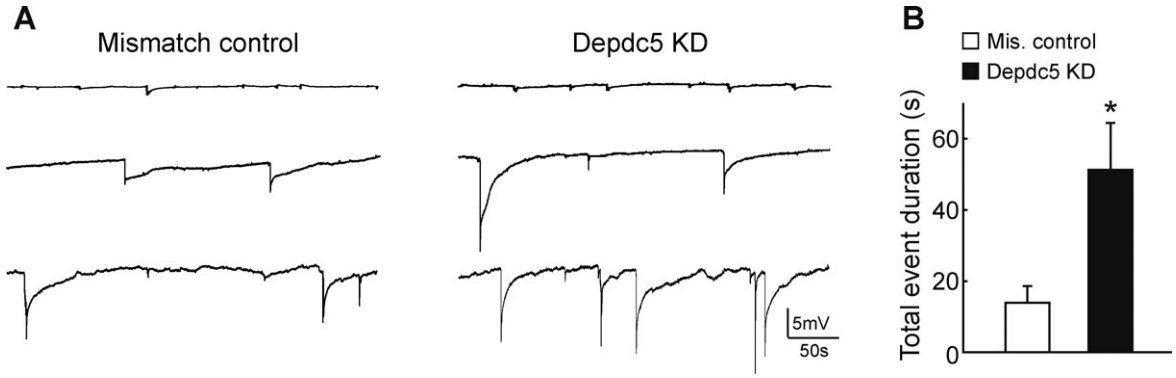

Figure 4. Electrophysiological extracellular recordings in the optic tectum of zebrafish larvae. (A) Representative traces of field recordings in the optic tectum for mismatch control and *depdc*5 knockdown larvae showing typical variations in the recorded electrical activity. Note the presence of spontaneous events in traces for either the mismatch controls and/or *depdc5* knockdowns. (B) Quantification of total event duration over the recording period of 1 h showing a significant increase in neuronal activity in the *depdc5* KD larvae as compared to controls.

(1 μmol/L) starting at the larval stage of 48 hpf. Motor ability scoring showed that the defects in locomotion associated with *depdc5* loss of function were still significantly improved by the rapamycin treatment when assessed at 72 hpf (see Fig. S2). These results indicate that pharmacological inhibition of mTORC1 can ameliorate the *depdc5* knockdown motor-related phenotype in zebrafish larvae.

Discussion

In this study, we developed a novel vertebrate model of *DEPDC5*, implicated in familial focal epilepsy with and without malformation of cortical development. Our model shows that *depdc5* knockdown leads to motor hyperactivity in 28 hpf embryos that persist at 48 hpf manifesting aberrant circular locomotion in zebrafish. The phenotypic features were significantly restored upon coexpression of the human *DEPDC5* cDNA, indicating the specificity of the motor phenotype due to *depdc5* knockdown as well as the functional conservation between human *DEPDC5* and *depdc5* zebrafish transcripts. *DEPDC5* mutations are predicted to cause loss of function, with the p.Arg239*, p.Arg487* and the p.Arg1087* point mutations shown to be specifically degraded by the nonsense-mediated mRNA decay in patient cell lines.[2,4] We selected a specific region in the protein that is highly conserved from zebrafish to humans to test the loss of function properties of *DEPDC5* mutations. Human *DEPDC5* cDNA constructs were generated carrying a nonsense mutation (p.Arg487*)[4] or a missense mutation (p.Arg485Gln) that was found to segregate with disease in patients with focal seizures[2] in order to define the pathogenicity of these mutations in vivo. Contrary to the WT protein, the two mutant *DEPDC5* did not result in any rescue of the hyperkinetic phenotype of the *depdc5* knockdown, supporting a loss of function mechanism. Moreover, *DEPDC5* mutants by themselves were unable to cause phenotypic features, arguing against gain of function properties of these mutant transcripts. This study allowed us to define the loss of function properties of one *DEPDC5* missense mutation alongside one nonsense mutation found in epileptic patients in vivo. Furthermore, in this report, we have performed all the necessary controls to validate the phenotype derived by knockdown through antisense morpholino oligonucleotides, including the use of both splice and ATG-blocking oligonucleotides, phenotypic rescue by the WT human cDNA, and injection of mismatch-oligo controls.[32,33]

Recent rodent knockout models of Depdc5 highlight the essential role of DEPDC5 during embryonic development, as constitutive null mutations result in embryonic lethality.[12,16] While the *Depdc5* heterozygous animals presented mTORC1 hyperactivation, they did not display any spontaneous seizures,[12,16] suggesting that in these constitutive *Depdc5* KO rodent models a functional compensation could partially mask the proepileptic effect of DEPDC5 loss of function. In the acute knockdown experiments presented here the possibility of functional compensation is strongly reduced. Indeed, a recent report in zebrafish comparing phenotypic features obtained upon knockdown and knockout approaches, showed important transcriptional alterations that could to mask the phenotype in the knockout, but not the knockdown conditions.[34] This highlights the importance of partial knockdown models in the functional validation of human mutations.

Of particular interest from a therapeutic point of view is the finding that in the Depdc5 homozygous null rat model, the embryonic lethality was rescued by rapamycin treatment,[12] highlighting the essential role that the DEPDC5-dependent regulation of mTOR plays in early

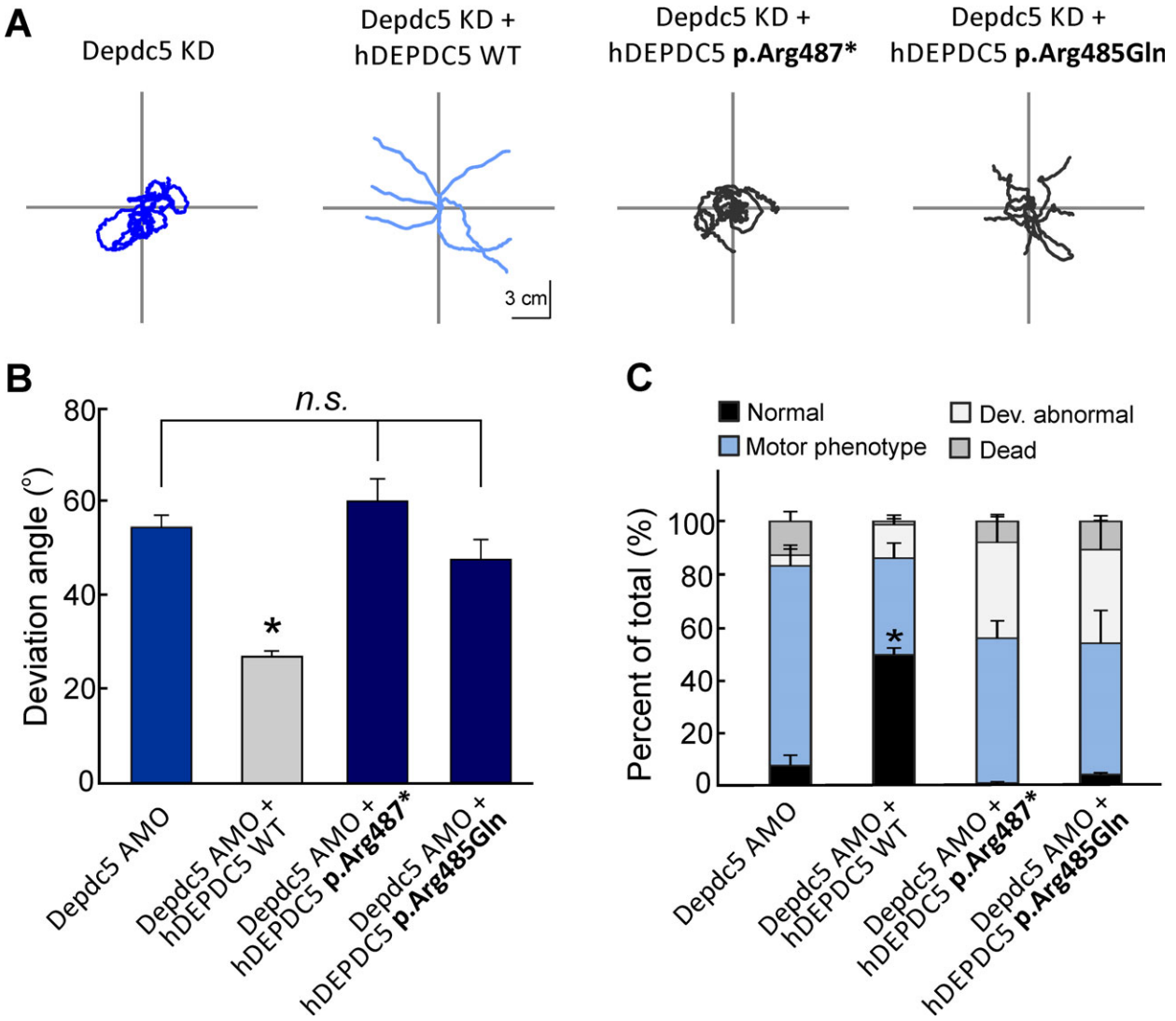

Figure 5. Human WT, but not mutant, *DEPDC5* can rescue the motor phenotype of Depdc5 knockdown zebrafish larvae at 48 hpf. (A) Overexpressing human WT *DEPDC5* alongside the ATG-targeting MO has a corrective effect on the tortuosity of the swimming trajectory associated with Depdc5 knockdown, as illustrated in these representative traces. However, overexpressing human *DEPDC5* transcripts carrying either of the two distinct epilepsy-related mutations fails to rescue the motor phenotype in Depdc5 KD. (B) Quantification of the tortuosity of the swimming trajectory by computing the deviation angle shows a significant rescue with WT, but not mutant human *DEPDC5* in the Depdc5 KD condition. (C) Bar graph showing a significant increase in the percentage of fish with normal phenotypes in Depdc5 KD with the introduction of human WT *DEPDC5* transcript as compared to Depdc5 KD alone. We did not observe any phenotypic rescue upon coexpression of the human mutant *DEPDC5* transcripts, the pArg487* and pArg485Gln.

development. The mTOR has been recently established as a major pathogenic pathway in the etiology of epilepsy.[35,36] DEPDC5 was described to act as a negative regulator of mTOR as part of the GATOR1 complex,[10,12] implicating that the loss-of-function of DEPDC5 would lead to an overactivation of the mTORC1 pathway. Indeed, we have found that treatment with rapamycin was effective at restoring the phenotypic features due to

Figure 6. Rapamycin treatment rescues the motor phenotype of Depdc5 knockdown larvae. (A) Representative swimming trajectories of 72 hpf Depdc5 KD larvae treated with DMSO or with rapamycin. (B). Quantification of the tortuosity of the swimming trajectory in 72 hpf Depdc5 KD and control larvae, treated with DMSO or rapamycin, showing a significant effect of rapamycin on the deviation angle of Depdc5 knockdown fish. C. Bar graph showing the motor score, on a scale from 0 to 5, attributed to 72 hpf larvae to describe their ability to swim in response to tail stimulation. Rapamycin treatment significantly improved the motor score of Depdc5 knockdown larvae.

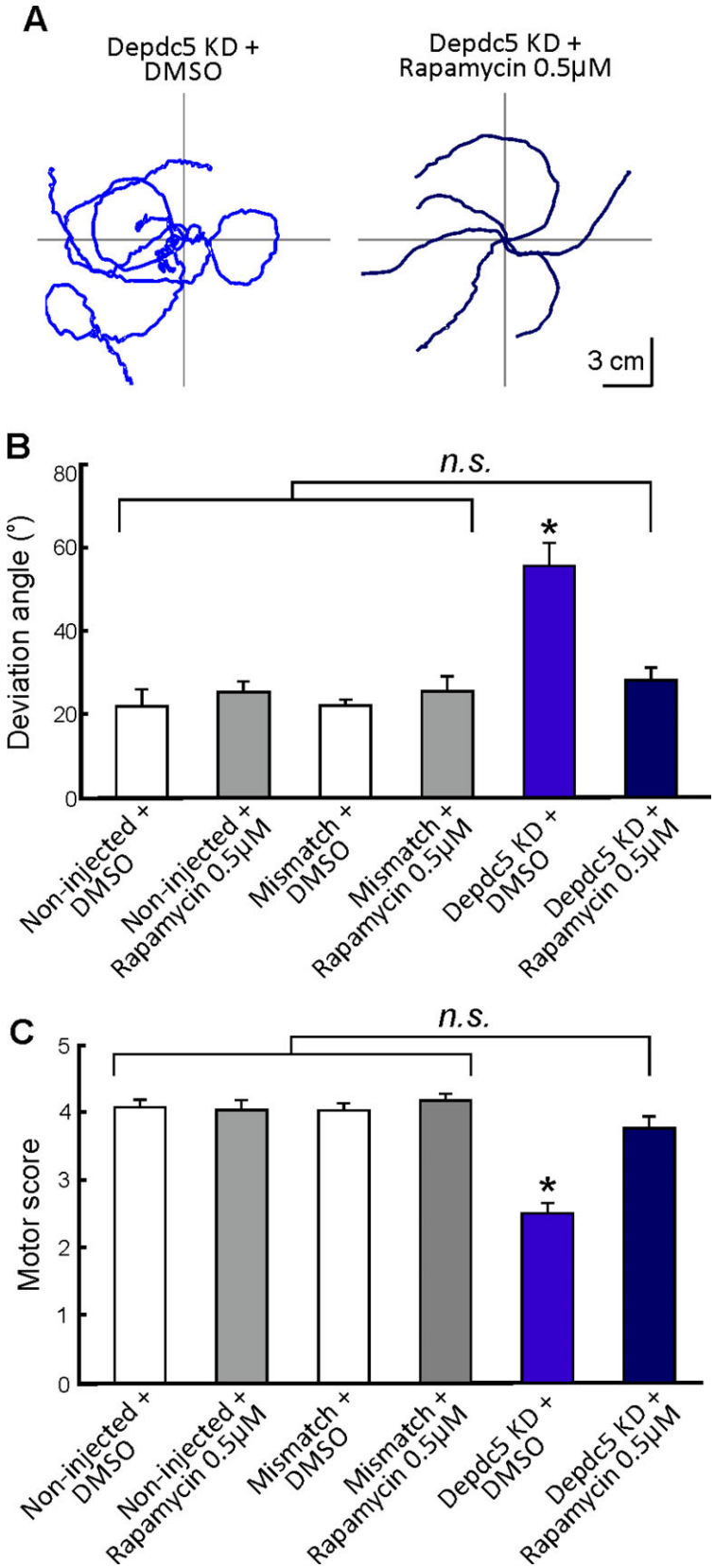

Depdc5 knockdown in zebrafish. Our results correlate well with a recent report showing the efficacy of rapamycin in rescuing phenotypic features in another mTORopathy model, the zebrafish homozygous null mutant for the tuberous sclerosis gene, tsc2.[25]

Reports of genetically and chemically induced zebrafish models of epilepsy (reviewed in 19,24,37,38), have established a number of behavioral paradigms that are used as metrics in this field. These measures are generally obtained at larval stages 3–7 dpf upon evoked or spontaneous swimming episodes.[20,21,28,39] Here we establish a novel measure of epilepsy-related hyperactivity at 28 hpf in the chorion, characterized by increased frequency of triggering stereotyped movements, such as coils and twitches (as defined in the text). This phenotype could be measured automatically by movement quantification and therefore could represent an early screening parameter for hyperactivity in zebrafish. At later stages of larval development, extensive research on both drug-induced and genetic models of epilepsy have revealed a stereotyped swimming characteristic of epileptogenic-like activity, where individual larvae swim in a circular, corkscrew-like trajectory.[20,22,24] To describe this particular phenotype, we have quantified the rotational angle of the swimming trajectory and obtained a reliable metric for comparing the epilepsy-like phenotypic features in zebrafish. Using this measurement, we demonstrate a clear deficiency of straight locomotion upon Depdc5 knockdown starting at 48 hpf, reproducibility of the phenotype using the splice AMO, as well as rescue of this phenotype by coexpressing WT *DEPDC5* cDNA.

Physiological recordings in the *Depdc5* knockdown zebrafish model showed an enhanced spontaneous activity in the optic tectum, similar to previous reports of zebrafish epilepsy models.[21,23,28] This electrical activity recorded at 4–6 dpf lacks, however, the characteristics of epileptiform activity that could be classified as typical ictal and interictal phases. In agreement, this model presented spontaneous seizure-like behavioral features in the earliest stages of embryonic development (28–48 hpf), whereas the later stages were characterized by abnormal swimming patterns. This could be due to a reduction in the severity of the phenotype as the effect of the translation blocking morpholino oligonucleotide is gradually reduced with time. *Depdc5* transcript expression by in situ hybridization revealed a potential role in cortical development, as strong labeling was revealed in the 24 hpf zebrafish brain (Fig. 1).

Therefore, the Depdc5 knockdown model developed in the versatile genetic organism, zebrafish, which presents an epilepsy-related phenotype, could prove to be particularly attractive for in vivo drug and genetic screening to identify modifiers of the mTOR pathway in order to provide therapeutic strategies for *DEPDC5* haploinsufficiency in patients.

Acknowledgments

The authors thank Anca Marian, Carine Dalle, and Feng Quan for technical assistance. Funding for this work was received from the Fédération pour la Recherche sur le Cerveau (FRC; SB and EK), AFM-Téléthon (18469 and 21488 for SC and 18462 for EK). Also support from a grant from Consiliul National al Cercetarii Stiintifice (CNCS) - ˇUnitatea Executiva pentru Finantarea Invatamantului Superior, a Cercetarii Dezvoltarii si Inovariiˇ (UEFISCDI) (RM), and the program "Investissements d'avenir" ANR-10-IAIHU-06 was obtained. HC (PLP20141031462) and EM (FDT20160736468) obtained PhD awards by the Fondation pour la Recherche Medicale.

Author Contribution

HC, EK, and SC designed the experimentation presented in this report and wrote the manuscript; HC and SC performed the genetic experimentation and phenotypic characterization presented in this article; AD and GD are responsible for the electrophysiological analysis and HT performed the in situ hybridization experimentation; EM and SI generated the *DEPDC5* mutant constructs and participated in the design of the study. SB and EK obtained funding for this project. All the authors listed have reviewed and revised this manuscript.

Conflicts of Interest

All the contributing authors declare no conflict of interest.

References

1. Scheffer IE, Berkovic S, Capovilla G, et al. ILAE classification of the epilepsies: position paper of the ILAE Commission for Classification and Terminology. Epilepsia 2017;58:512–521.
2. Ishida S, Picard F, Rudolf G, et al. Mutations of DEPDC5 cause autosomal dominant focal epilepsies. Nat Geo 2013;45:552–555.
3. Dibbens LM, de Vries B, Donatello S, et al. Mutations in DEPDC5 cause familial focal epilepsy with variable foci. Nat Genet 2013;45:546–551.
4. Picard F, Makrythanasis P, Navarro V, et al. DEPDC5 mutations in families presenting as autosomal dominant nocturnal frontal lobe epilepsy. Neurology 2014;82:2101–2106.
5. Ricos MG, Hodgson BL, Pippucci T, et al. Mutations in the mammalian target of rapamycin pathway regulators NPRL2 and NPRL3 cause focal epilepsy. Ann Neurol 2016;79:120–131.

6. Baulac S, Ishida S, Marsan E, et al. Familial focal epilepsy with focal cortical dysplasia due to DEPDC5 mutations. Ann Neurol 2015;77:675–683.
7. Scerri T, Riseley JR, Gillies G, et al. Familial cortical dysplasia type IIA caused by a germline mutation in DEPDC5. Ann Clin Transl Neurol 2015;2:575–580.
8. D'Gama AM, Geng Y, Couto JA, et al. Mammalian target of rapamycin pathway mutations cause hemimegalencephaly and focal cortical dysplasia. Ann Neurol 2015;77:720–725.
9. Baulac S, Weckhuysen S. DEPDC5-Related Epilepsy. In: Adam MP, Ardinger HH, Pagon RA, Wallace SE, Bean LJH, Stephens K, Amemiya A, eds. GeneReviews® [Internet]. Seattle (WA): University of Washington, Seattle, 1993-2018. (Accessed September 29, 2016)
10. Bar-Peled L, Chantranupong L, Cherniack AD, et al. A Tumor suppressor complex with GAP activity for the Rag GTPases that signal amino acid sufficiency to mTORC1. Science 2013;340:1100–1106.
11. Panchaud N, Péli-Gulli M-P, De Virgilio C. Amino acid deprivation inhibits TORC1 through a GTPase-activating protein complex for the Rag family GTPase Gtr1. Sci Signal 2013;6:ra42. Available from: https://doi.org/10.1126/scisignal.2004112 (Accessed May 28, 2013)
12. Marsan E, Ishida S, Schramm A, et al. Depdc5 knockout rat: a novel model of mTORopathy. Neurobiol Dis 2016;89:180–189.
13. Sim JC, Scerri T, Fanjul-Fernández M, et al. Familial cortical dysplasia caused by mutation in the mammalian target of rapamycin regulator NPRL3. Ann Neurol 2016;79:132–137.
14. Weckhuysen S, Marsan E, Lambrecq V, et al. Involvement of GATOR complex genes in familial focal epilepsies and focal cortical dysplasia. Epilepsia 2016;6:1–10.
15. Korenke GC, Eggert M, Thiele H, et al. Nocturnal frontal lobe epilepsy caused by a mutation in the GATOR1 complex gene NPRL3. Epilepsia 2016;57:e60–e63.
16. Hughes J, Dawson R, Tea M, et al. Knockout of the epilepsy gene Depdc5 in mice causes severe embryonic dysmorphology with hyperactivity of mTORC1 signalling. Sci Rep 2017;7:12618.
17. Yuskaitis CJ, Jones BM, Wolfson RL, et al. A mouse model of DEPDC5 related epilepsy: neuronal loss of Depdc5 causes dysplastic and ectopic neurons, increased mTOR signaling, and seizure susceptibility. Neurobiol Dis 2017;111:91–101.
18. Fallis A. Perspectives of zebrafish models of epilepsy: what, how and where next? J Chem Inf Model 2013;53:1689–1699.
19. Hortopan GA, Dinday MT, Baraban SC. Zebrafish as a model for studying genetic aspects of epilepsy. Dis Model Mech 2010;3:144–148.
20. Baraban SC, Taylor MR, Castro PA, Baier H. Pentylenetetrazole induced changes in zebrafish behavior, neural activity and c-fos expression. Neuroscience 2005;131:759–768.
21. Teng Y, Xie X, Walker S, et al. Knockdown of zebrafish lgi1a results in abnormal development, brain defects and a seizure-like behavioral phenotype. Hum Mol Genet 2010;19:4409–4420.
22. Grone BP, Marchese M, Hamling KR, et al. Epilepsy, behavioral abnormalities, and physiological comorbidities in syntaxin-binding protein 1 (STXBP1) mutant zebrafish. PLoS ONE 2016;11:1–25.
23. Baraban SC, Dinday MT, Hortopan GA. Drug screening in Scn1a zebrafish mutant identifies clemizole as a potential Dravet syndrome treatment. Nat Commun 2013;4:2410.
24. Suls A, Jaehn JA, Kecskés A, et al. De novo loss-of-function mutations in CHD2 cause a fever-sensitive myoclonic epileptic encephalopathy sharing features with dravet syndrome. Am J Hum Genet 2013;93:967–975.
25. Scheldeman C, Mills JD, Siekierska A, et al. mTOR-related neuropathology in mutant tsc2 zebrafish: phenotypic, transcriptomic and pharmacological analysis. Neurobiol Dis 2017;108:225–237.
26. Kimmel CB, Ballard WW, Kimmel SR, et al. Stages of embryonic development of the zebrafish. Dev Dyn 1995;203:253–310.
27. Quan FB, Dubessy C, Galant S, et al. Comparative distribution and in vitro activities of the urotensin II-related peptides URP1 and URP2 in zebrafish: evidence for their colocalization in spinal cerebrospinal fluid-contacting neurons. PLoS ONE 2015;10:e0119290.
28. Afrikanova T, Serruys ASK, Buenafe OEM, et al. Validation of the Zebrafish pentylenetetrazol seizure model: locomotor versus electrographic responses to antiepileptic drugs. PLoS ONE 2013;8:e54166.
29. Drapeau P, Saint-Amant L, Buss RR, et al. Development of the locomotor network in zebrafish. Prog Neurobiol 2002;68:85–111.
30. Saint-Amant L, Drapeau P. Synchronization of an embryonic network of identified spinal interneurons solely by electrical coupling. Neuron 2001;31:1035–1046.
31. Teng Y, Xie X, Walker S, et al. Loss of zebrafish lgi1b leads to hydrocephalus and sensitization to pentylenetetrazol induced seizure-like behavior. PLoS ONE 2011;6:e24596.
32. Eisen JS, Smith JC. Controlling morpholino experiments: don't stop making antisense. Development 2008;135:1735–1743.Available from: http://dev.biologists.org/cgi/doi/10.1242/dev.001115
33. Stainier DYR, Raz E, Lawson ND, et al. Guidelines for morpholino use in zebrafish. PLoS Genet 2017;13:e1007000.
34. Rossi A, Kontarakis Z, Gerri C, et al. Genetic compensation induced by deleterious mutations but not gene knockdowns. Nature 2015;13:230–233.Available from: http://www.ncbi.nlm.nih.gov/pubmed/26168398
35. Crino PB. mTOR signaling in epilepsy: insights from malformations of cortical development. Cold Spring Harb Perspect Med 2015;5:a022442.

36. Baulac S. mTOR signaling pathway genes in focal epilepsies. Prog Brain Res 2016;226:79.
37. Cunliffe VT. Building a zebrafish toolkit for investigating the pathobiology of epilepsy and identifying new treatments for epileptic seizures. J Neurosci Methods 2016;260:91–95.
38. Grone BP, Baraban SC. Animal models in epilepsy research: legacies and new directions. Nat Neurosci 2015;18:339–343.Available from: https://doi.org/10.1038/nn.3934
39. Mussulini BHM, Leite CE, Zenki KC, et al. Seizures induced by pentylenetetrazole in the adult zebrafish: a detailed behavioral characterization. PLoS ONE 2013;8:e54515.

Supporting Information

Additional Supporting Information may be found online in the supporting information tab for this article:

Table S1. The majority of genes encoding major players involved in the autophagy pathway are well conserved from zebrafish to human.
Figure S1. Depedc5 knockdown does not affect the gross morphology of zebrafish embryos.
Figure S2. Rapamycin treatment is effective when started at 48 hpf.
Videos S1. Aberrant coiling upon Depdc5 knockdown.
Video S2. Upon Depdc5 knockdown we observed an increased frequency of coiling and twitching and seizure-like activity in a percentage of embryos.
Video S3. Control conditions showing normal evoked swimming at 48-hour post fertilization.
Video S4. Depdc5 knockdown zebrafish display tortuous, cork-screw swimming bouts.

